Applied Catalysis A: General 467 (2013) 235–245

Contents lists available at ScienceDirect

Applied Catalysis A: General

journal homepage: www.elsevier.com/locate/apcata

n-Decane dehydrogenation on Pt, PtSn and PtGe supported on spinels prepared by different methods of synthesis

Adriana D. Ballarini *, Sergio R. de Miguel, Alberto A. Castro, Osvaldo A. Scelza

Instituto de Investigaciones en Catálisis y Petroquímica (INCAPE), Facultad de Ingeniería Química (Universidad Nacional del Litoral)-CONICET, Santiago del Estero 2654, S3000AOJ Santa Fe, Argentina

ARTICLE INFO

Article history:
Received 22 March 2013
Received in revised form 28 June 2013
Accepted 14 July 2013
Available online 23 July 2013

Keywords:
Spinel
Zinc aluminate
PtSn and PtGe catalysts
Mechanochemical synthesis
Coprecipitation

ABSTRACT

The catalytic performance of Pt, PtSn and PtGe supported on $ZnAl_2O_4$ obtained by mechanochemical synthesis (MS) or coprecipitation (COPR) is studied in the production of 1-decene from the n-decane dehydrogenation. The effect of preparation methods and Sn and Ge addition to Pt on the activity and selectivity was analyzed. The catalytic characterization was carried out by using XRD, Specific surface area, 2-propanol dehydration reaction, equilibrium pH, cyclohexane dehydrogenation (CHD), cyclopentane hydrogenolysis (CPH), TPR, H_2 chemisorption, XPS, TPO, and TEM. Characterization studies indicate that the addition of Sn to the Pt metal phase modifies not only the catalytic properties, but deactivation and stability as well. PtSn catalysts on both spinels were more active, with lower activity fall than PtGe ones and the higher the Sn loading, the more noticeable this effect. Besides, PtSn catalysts supported on $ZnAl_2O_4$ MS showed a more stabilizing effect.

1. Introduction

Olefins are very important raw materials in the petrochemical and petroleum refining industries due to their applications in several processes. One application of α-monoolefins of high molecular weight is in the production of biodegradable detergents or tensoactives. This industry has become very important as well, since dodecylbenzene was found to have better properties than soaps. These detergents were initially produced by alkylation of benzene with tetramers of propene (a mixture of C_{10}–C_{12} highly branched olefins) followed by sulfonation and neutralization with NaOH. This process had the problem of the lack of biodegradability of the detergents [1,2]. A new process that appeared in the mid 60s, was the production of sodium alkylbenzenesulfonate. This compound has an aliphatic linear chain of C_{10}–C_{14} [3,4] which allows a fast biodegradation. These biodegradable detergents are obtained by alkylation of benzene with linear α-monoolefins of C_{10}–C_{14}. The production of the biodetergents at industrial scale was successful, thus displacing the preceding technologies. In this way the production of linear alkylbenzene or linear alkylbenzene sulfonate (LAB or LABS) increased significantly [3,4].

This paper studies the production of 1-decene from the n-decane catalytic dehydrogenation. The dehydrogenation of high paraffins to the corresponding n-monoolefins can take place on noble metals (Group 10) like Pt. This reaction is normally accompanied by undesirable side ones such as hydrogenolysis, cracking, aromatization and coke formation. In consequence, it is very important to analyze the addition of modifiers (elements of the Group 14 like Sn and Ge), which can affect the activity, selectivity and stability of the catalysts [3–10]. Furthermore the coke deposition can be diminished by using H_2 in the feed [11]. In the present paper monometallic (Pt) and bimetallic (PtSn and PtGe) catalysts supported on $ZnAl_2O_4$ obtained by both mechanochemical synthesis (MS) or coprecipitation (COPR) are evaluated in the n-decane dehydrogenation. The specific surface area of $ZnAl_2O_4$ can be improved choosing the appropriate synthesis method. In general, there are several preparation methods of $ZnAl_2O_4$ spinels, for example solid state-reaction or ceramic method [12–19] or wet chemical routes such as precipitation or coprecipitation [12–14,20–24], sol–gel [12–14,25–28] and other methodologies like hydrothermal methods [29–33], combustion in aqueous solution [34], molten salts synthesis [35], etc. These techniques try to reduce the severity of the thermal treatments, thus achieving a material of higher specific area and higher chemical purity. It must be noted that the comparison of the catalytic behavior of monometallic catalysts supported on the $ZnAl_2O_4$ spinel prepared by COPR, MS and ceramic method (CM) was previously reported in the bibliography by Ballarini et al. [36]. The Pt catalysts prepared with $ZnAl_2O_4$ COPR presented better activity and selectivity (in the reaction of n-butane dehydrogenation) than the ones prepared with $ZnAl_2O_4$ MS and $ZnAl_2O_4$ CM, and this could be correlated with a higher metallic dispersion and lower particle sizes, detected by H_2 chemisorption and TEM, respectively. For this

* Corresponding author. Tel.: +54 342 455 5279; fax: +54 342 453 1068.
E-mail address: aballa@fiq.unl.edu.ar (A.D. Ballarini).

0926-860X/$ – see front matter © 2013 Published by Elsevier B.V.
http://dx.doi.org/10.1016/j.apcata.2013.07.030

reason, in this paper, $ZnAl_2O_4$ prepared by mechanochemical synthesis and coprecipitation was used as support of metallic catalysts for paraffin dehydrogenation.

With reference to this topic, there are no papers in the open literature about bimetallic catalysts supported on $ZnAl_2O_4$ for n-decane dehydrogenation, specially the use of couples composed of Pt and Ge on these supports. It must be remembered that $ZnAl_2O_4$ has a spinel structure which is appropriated for this reaction type due to the high thermal stability, neutral acid-base characteristic and low Pt sintering rate since there is a strong metal–support interaction [37–39]. Bhasin et al. [40] studied that the unmodified alumina-supported platinum catalysts are highly active but not selective to dehydrogenation. They showed a simple reaction scheme for light paraffins dehydrogenation, but the complexity of the reaction increases when the number of C atoms in the reactant increases.

In this paper the effect of the Sn or Ge loading added to Pt is also studied, in order to correlate the properties of the support with the physicochemical characteristics of the catalysts and the catalytic properties.

2. Experimental

In the mechanochemical synthesis of the $ZnAl_2O_4$ (MS), γ-Al_2O_3 (CK 300, 99.9% from Cyanamid Ketjen) and ZnO (AnalaR, 99.7%) were ground until fine powder and they were mixed in a stoichometric ratio. Then distilled water was added in order to produce a paste. The paste was ground by using a grinded that consists of a teflon® cylinder of 140 mL and zirconia balls with a diameter of 13 mm. The cylinder rotated at 200 rpm in contact with air at room temperature for 12 h. The paste thus obtained was dried at 120 °C and calcined at 900 °C for 12 h. After obtained the precursor of $ZnAl_2O_4$, a purification step was achieved by washing the precursors with $(NH_4)_2CO_3$ 1 M to eliminate residues of ZnO. The ratio volumen of solution/mass of solid was 1.5 mL/g.

$ZnAl_2O_4$ COPR was prepared by coprecipitation of the two metallic ions (Zn and Al) at variable pH. The precipitation was made by using $Al(NO_3)_3{\cdot}9H_2O$, Baker, 98.9% and $Zn(NO_3)_2{\cdot}6H_2O$, Baker, 99,0%. Finally the pH was adjusted at 7.5 by using a $NH_4(OH)$ 50% (v/v). After precipitation under stirring at 50 °C a gel is obtained. This gel was aged for 24 h and then washed with distilled water until total elimination of ammonia. Finally it was dried at 120 °C and calcined at 800 °C under air flow for 8 h.

The different samples (powders) of the support were analyzed in a XRD Diffractometer Shimadzu using a CuKα radiation, voltage: 30 kV, current: 30 mA, divergence and dispersion: 2°, using the following diffraction angle range: 10–80°, and scanning in a continuous way.

The determination of specific surface area and pore volume was carried out by using an Accusorb equipment, Model 2100 E from Micromeritics. Samples were outgassed at 200 °C and 10^{-4} mmHg for 2 h. The dead volume was determined by using He (from AGA, 99.999%) at the temperature of liquid N_2 (77 K). N_2 isotherms were obtained at 77 K.

The 2-propanol dehydration reaction (used for the measurement of the acid character of the samples) was made in a continuous flow reactor at atmospheric pressure. 2-propanol was vaporized in a H_2 flow (H_2/2-propanol molar ratio = 19) and it was fed with a space velocity of 0.52 mol alcohol h^{-1} g cat^{-1}. Catalysts were previously reduced "in situ" at 500 °C for 3 h under flowing H_2. The mass of the sample was 0.100 g, the reaction temperature was 210 °C and feeding flow was 600 mL min^{-1}. The reaction products were analyzed by GC using a Carbowax 20 column, 2 m length × 1/8".

The determination of equilibrium pH of the aqueous suspension of the support (10 mL water g of $support^{-1}$) was performed following the technique reported by Román-Martínez et al. [41]. The suspension was stirred and the pH was measured until it reached a constant value.

The monometallic Pt (0.3 wt.%) catalyst was prepared by impregnation (6 h, 25 °C) of the corresponding support ($ZnAl_2O_4$ MS and $ZnAl_2O_4$ COPR) with an aqueous solution of H_2PtCl_6 (Aldrich 99%). The concentration of the H_2PtCl_6 solution was such as to obtain the desired Pt loading. The impregnating volume/support weight ratio was 1 mL g^{-1} for $ZnAl_2O_4$ MS and 0.7 mL g^{-1} for $ZnAl_2O_4$ COPR. After 6 h, the samples were dried at 120 °C for 12 h and calcined in air at 500 °C for 3 h.

Bimetallic PtSn catalysts were obtained by impregnation of the monometallic Pt catalyst (previously dried) with a $SnCl_2$ solution (in an HCl 1.2 M medium). In all the cases the Pt concentration was 0.3 wt.%. The Sn concentrations in the impregnating solution were 0.0253 and 0.042 mol L^{-1} Sn for 0.3 and 0.5 wt.% loading, respectively. After impregnation with Sn, samples were dried at 120 °C for 12 h.

Bimetallic Pt-Ge catalysts were also obtained by impregnation of the monometallic Pt catalyst (previously dried) with an aqueous solution of $GeCl_4$ (dissolved in HCl 1M). The Pt concentration in the catalysts was 0.3 wt.%. The Ge concentrations in the impregnating solutions were 0.025 and 0.04 mol L^{-1} for the Ge loading of 0.18 and 0.3 wt.%, respectively. After impregnation with Ge the samples were dried at 120 °C for 12 h. Finally bimetallic samples were calcined at 500 °C for 3 h under flowing air.

TPR experiments of the catalysts were carried out at atmospheric pressure and using a reductive mixture of H_2-N_2 (5% H_2 v/v, 10 cm^3 STP min^{-1}), and a heating linear programming rate of the sample (0.300 g) equal to 6 K min^{-1} from room temperature up to 700 °C. Before the TPR measurements the samples were calcined "in situ" at 500 °C with flowing air 160 mL min^{-1} g cat^{-1} for 3 h.

The H_2 chemisorption was performed at 25 °C in a static volumetric equipment. The sample used in the experiments ranged between 0.300 and 0.500 g. In these experiments the catalysts were previously reduced in H_2 at 500° C for 2 h, then outgassed under high vacuum (10^{-5} Torr) at the same temperature for 2 h and finally cooled down to room temperature. The H_2 adsorption isotherms were performed at room temperature between 0 and 100 Torr. The isotherms were linear in the range of used pressures and the H_2 chemisorption capacity was calculated by extrapolation of the isotherms to zero pressure.

The cyclohexane (CH) dehydrogenation reaction was carried out in a differential flow reactor fed at 6 mL h^{-1} with a H_2 – CH mixture (H_2/CH molar ratio = 26). Previous to the reaction the catalysts were reduced "in situ" under flowing H_2 at 500 °C for 3 h at the reaction temperature indicated in each case. The reaction products were analyzed by GC using a Chromosorb column at 60 °C. The activation energies were obtained from the slope of the curve ln R^0 vs $1/T$ (T – temperature, K). R^0 was calculated from the conversion obtained at three different temperatures. The sample mass was chosen to obtain a conversion less than 5%, condition in which the reactor can be considered as a differential one. For the cyclopentane (CP) hydrogenolysis reaction, the catalyst samples were previously reduced "in situ" under flowing H_2 at 500 °C for 3 h. The reaction was performed in a differential flow reactor fed at 6 mL h^{-1} with H_2 – CP mixture (H_2/CP molar ratio = 26). The reaction temperature was 500 °C. The reaction products were analyzed by GC using a Chromosorb column at 25 °C.

The XPS spectra were obtained in a spectrometer Specs, by using MgKα or AlKα (for Ge determination at high BE) sources at 1253.6 or 1486.6 eV, respectively. Other conditions were: power of 100 W (10 kV and 10 mA) and the pressure of the analysis chamber was 4.10^{-10} Torr. Before XPS, samples were previously reduced in H_2 at 530 °C for 3 h. The BE were referred to the Al2p peak (74 eV). Spectra were obtained by using the SpecsLab software. The peak areas

Table 1
Specific surface area (S_{BET}) and pore volume of $ZnAl_2O_4$ prepared by different methods.

	MS	COPR
S_{BET} ($m^2\,g^{-1}$)	21	40
V_{pore} ($mL\,g^{-1}$)	0.053	0.118

were estimated by means of a combination of Lorentzian-Gaussians curves in a different proportion and using Casa XPS software.

Transmission electron micrographs of the reduced catalysts were taken by using a JEOL 100CX microscope with a nominal resolution of 6 Å, operated with an acceleration voltage of 100 kV, and magnification ranges of 80,000× and 100,000×. The specimens were introduced into the microscope column. For each catalyst, a very important number of Pt particles were observed and the distribution curves of particle sizes were done.

To quantify the carbonaceous deposits, the profiles of temperature-programmed oxidation before and after the n-decane dehydrogenation reaction were determined using the thermogravimetric analysis (TGA) technique. The experiments were carried out on the SDTA Mettler STAR^e. Fresh (used as a reference) and used catalysts were stabilized under N_2 flow at 250 °C for 1 h before starting the TPO experiments. The samples (0.010 g) were heated at 5 °C min^{-1} from 250 to 500 °C under air flow.

The n-decane dehydrogenation reaction was carried out in a flow reactor. The reactive mixture (n-C_{10}-H_2) is prepared "in situ" in the desired proportion by using a mass flow control for H_2 and a Sage syringe pump for n-C_{10}. This mixture was vaporized before injected to the reactor. All the gases were high purity (99.95% minimum) ones. The liquid effluent obtained by condensation of the outlet of the reactor was analyzed in a Varian STAR 3400 CX chromatograph with a FID detector and a capillary column CP-Sil-PONA CB, 50 m length, 0.2 mm diameter and 0.5 μm of the film thickness. The working temperature of the column was 250 °C.

In order to determine the conversion and selectivity values, fractions of the liquid product were sampled at 10 min of the reaction beginning and then at intervals of 15 min until 130 min of total reaction time. By using the chromatographic analysis, five groups of compounds were identified according to the retention time:

(1) Light paraffins of C_5–C_{10} from the cracking reactions, **[<C_{10}].**
(2) n-decane (used as reference peak), **[n-C_{10}].**
(3) 1-decene or α-monoolefin of C_{10}, **[1-C_{10}** =].
(4) Others monoolefins (positional isomers) and conjugated diolefins and not conjugated, n-dienes, n-trienes,**[$C_{10=}$]** (except 1-decene).
(5) Non linear chains including ramified chains, isoparaffins, isoolefins, cyclization products, aromatics, alkyl aromatics, etc.), **[i-c-C_{10}]**.

It must be indicated that in all cases the liquid yield (<C_5) was in the range of 97–98%. In previous experiments it was found that a feeding of a mixture of n-decane and hydrogen with a $H_2/C_{10}H_{22}$ = 4 molar ratio decreased the catalyst deactivation that allows the reaction evolution to be controlled. Other operating conditions were: T = 465 °C, P = 1 atm, LHSV (h^{-1}) = 40 and weigth of catalyst = 0.35 g.

The n-decane conversion was calculated as the sum of the percentages of the chromatographic areas of all the reaction products affected by the corresponding response factors, except for H_2.

The selectivities to different group of products (j) were defined as follows:

S_j = mol product/Σ mol product j (except H_2).

The yield to 1-decene was defined as:

$Y_{\mathbf{1\text{-}decene}}$ = conversion × selectivity to 1-decene.

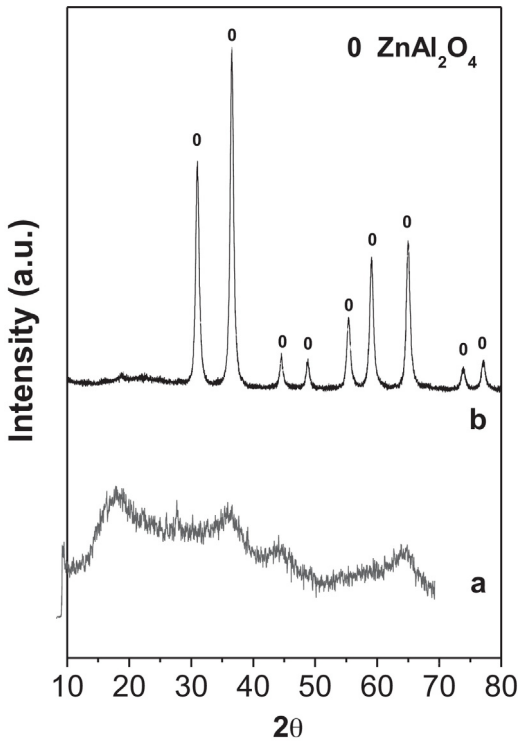

Fig. 1. XRD of the $ZnAl_2O_4$ obtained by coprecipitation. (a) Precursor and (b) precursor calcined at 800 °C.

Conversions, selectivities and yields were calculated at different reaction times (10–130 min). It is worth noticing that even though the catalysts were tested at conversions between 2 and 13%, no important selectivity changes were obtained at different conversions.

3. Results and discussion

3.1. Characterization of supports

Table 1 shows the results of specific surface area (S_{BET}) and pore volumen (V_{pore}) of $ZnAl_2O_4$ prepared by different methods. It can be observed that the S_{BET} of the $ZnAl_2O_4$ COPR is about two times higher than $ZnAl_2O_4$ MS one. These supports were treated under milder conditions than $ZnAl_2O_4$ prepared by the ceramic method, which displayed a lower specific surface area (about 11 $m^2\,g^{-1}$) [36]. It must be noted that assuming a Gaussian distribution of pore sizes, the average pore sizes are similar for $ZnAl_2O_4$ COPR and $ZnAl_2O_4$ MS.

Fig. 1 shows the XRD spectra after each step of the preparation of $ZnAl_2O_4$ COPR. The XRD of the precursor shows the presence of an amorphous solid (Fig. 1a) and after calcination at 800 °C, it clearly shows a spinel structure [42] without impurities (Fig. 1b).

Fig. 2 shows the XRD patterns of the precursor obtained by MS (2a), calcined precursor (2b) and purified sample (after drying with aqueous solution of ammonium carbonate) (2c). Fig. 2a displays only peaks corresponding to ZnO and γ-Al_2O_3. After calcination, characteristic peaks of $ZnAl_2O_4$ are mainly produced and small lines (traces) of ZnO and γ-Al_2O_3 (Fig. 2b). When the calcined precursor is purified, only XRD lines of $ZnAl_2O_4$ are detected (Fig. 2c). In all calcined samples the XRD peaks of $ZnAl_2O_4$ are related to the following planes: (2 2 0), (3 1 1), (4 0 0), (3 3 1), (4 2 2), (5 1 1), (4 4 0), (6 2 0) and (5 3 3).

Fig. 3 shows the activity results in 2-propanol dehydration reaction for the two $ZnAl_2O_4$ and the γ-Al_2O_3 (used as reference). In

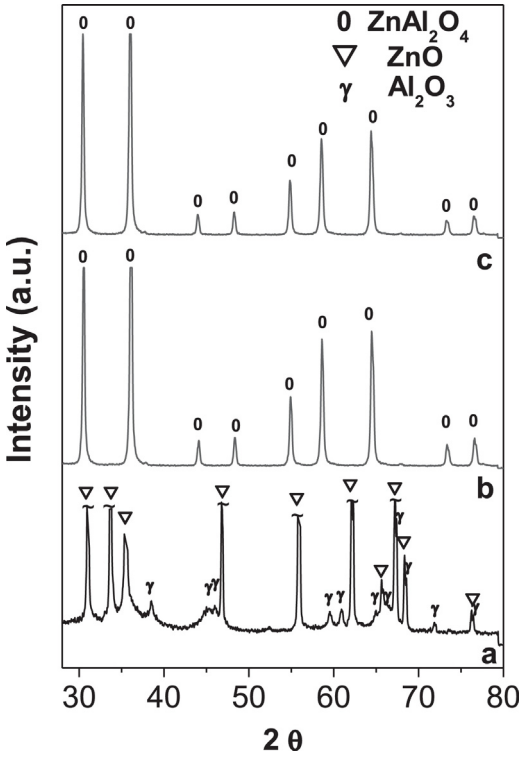

Fig. 2. (a) XRD of a mixture between ZnO and γ-Al_2O_3 submitted to a wet grinded (12 h) after calcination (without purification) and (c) after purification (c).

all cases the reaction produces propylene. It must be noted that γ-Al_2O_3 has Lewis acidity [43] and subsequently the 2-propanol conversion is high (about 20%). With reference to $ZnAl_2O_4$ samples, they show a lower dehydration capacity, evidenced by the low acidity of these supports. However $ZnAl_2O_4$ COPR shows a slightly higher conversion than $ZnAl_2O_4$ MS, and consequently the last sample has the lowest acidity.

Equilibrium pHs of the spinels obtained by different methods were 8.2–8.6, these values being in agreement with the very low acid character [44] of the supports according to the dehydration of 2-propanol reaction results.

3.2. Characterization of the metallic phase

Tables 2 and 3 show initial rate (R^0_{CH}) and activation energy values for cyclohexane dehydrogenation reaction at 400 °C (structure-insensitive reaction [45,46]) and also initial reaction values from cyclopentane hydrogenolysis reaction (R^0_{CP}) at 500 °C

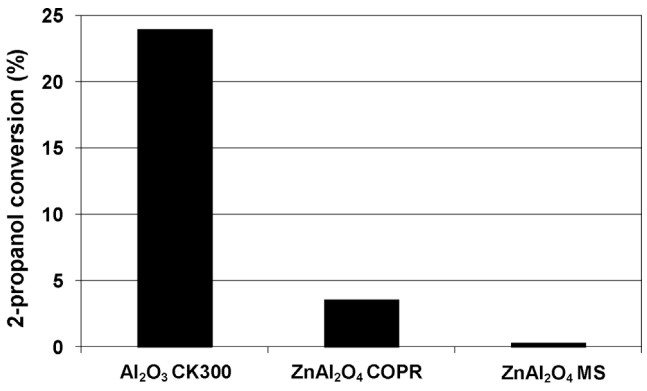

Fig. 3. 2-propanol conversion in the dehydration reaction for γ-Al_2O_3 (reference), $ZnAl_2O_4$ COPR and $ZnAl_2O_4$ MS.

(structure sensitive reaction) [47–49] for Pt, PtSn and PtGe catalysts supported on $ZnAl_2O_4$ MS and $ZnAl_2O_4$ COPR. When a second metal is added to a Pt catalyst, two effects can take place, viz, the geometric one, this being the blocking and/or dilution of the Pt active atoms by the second metal, and the electronic one that modifies the electronic structure of the Pt. It can be observed From Tables 2 and 3 that monometallic catalysts supported on $ZnAl_2O_4$ MS and $ZnAl_2O_4$ COPR show similar activation energy values. The Sn or Ge addition increases the activation energy, this indicating a certain electronic modification of the metallic phase probably by alloy formation. This electronic effect seems to be more pronounced for Sn containing catalysts than Ge containing ones when $ZnAl_2O_4$ MS is used as support. For $ZnAl_2O_4$ COPR series there are small differences in the activation energies. Besides, the second metal addition decreases R^0_{CH} values in about one order of magnitude. It can be concluded that the addition of either Sn or Ge to Pt/$ZnAl_2O_4$ catalysts decreases the dehydrogenation activities thus showing a blocking geometric effect by Sn or Ge that decreases the number of exposed Pt atoms and also electronic effects as it was above mentioned.

On the other hand, the cyclopentane hydrogenolysis reaction is influenced by the size and structure of the metallic particles. Besides a special arrangement of surface active atoms are needed for this reaction to take place [50]. Results of this reaction are shown in Tables 2 and 3. Monometallic catalysts supported on both $ZnAl_2O_4$ supports show hydrogenolytic activities only from 500 °C so it could be explained that these supports produce metallic structures with low density of edges and corners (active centers for this reaction) [21,51]. In bimetallic catalysts supported on $ZnAl_2O_4$ MS or $ZnAl_2O_4$ COPR the second metal addition inhibits the hydrogenolytic reaction. This can be due not only to an electronic modification of Pt by Sn or Ge but also geometric effects. Sn or Ge addition decreases the concentration of metallic ensembles that the cyclopentane hydrogenolysis needs. Summarizing the results of both test reactions, the second metal introduces both geometric and electronic modifications in the metallic phase.

Fig. 4a and b shows the TPR profiles of PtSn (0.3 and 0.5 wt.%) catalysts supported on $ZnAl_2O_4$ MS and $ZnAl_2O_4$ COPR. Monometallic Pt and Sn catalysts are also added for comparison. Fig. 5 shows the TPR profiles of PtGe (0.18 and 0.3 wt.%) catalysts supported on $ZnAl_2O_4$ MS (a) and $ZnAl_2O_4$ COPR (b). The profiles of the monometallic catalysts are also included. Zinc aluminate is not reduced in the used range of temperature (25–700 °C) [14]. Fig. 4a shows that the Pt/$ZnAl_2O_4$ MS catalyst gives a well-defined reduction peak at 260 °C, whereas the corresponding peak of Pt/$ZnAl_2O_4$ COPR is wider and it appears at about 300 °C. These peaks would be caused by the reduction of oxychloride compounds formed during the impregnation with H_2PtCl_6 and successive thermal treatments [52]. The shift to higher temperatures for the $ZnAl_2O_4$ COPR-supported catalysts could be due both to smaller particle sizes and the modification of the Pt-support interaction [14]. For both supports, the Sn(0.5)/$ZnAl_2O_4$ catalyst profile shows a small but very wide reduction zone from 200 to 250 °C to higher temperatures. In bimetallic PtSn/$ZnAl_2O_4$ catalysts, the main reduction peak of Pt is placed at 280–300 °C for the $ZnAl_2O_4$ MS support and at about 300 °C for the $ZnAl_2O_4$ COPR one. These shifts in the reduction temperature with respect to Pt monometallic catalysts together with certain widening of the peak could be attributed to a co-reduction of both metals that would form Pt-Sn alloys. Another wide and small peak at about 500–550 °C was observed, and it could correspond to the reduction of SnO*x* species. In PtSn/$ZnAl_2O_4$ COPR catalysts the same TPR peaks are observed, but shifted to higher temperature. The peak at 550 °C could be also due to the reduction of small quantities of free SnO*x* species stabilized in the support.

Fig. 5a and b shows TPR profiles of PtGe supported on $ZnAl_2O_4$ MS and $ZnAl_2O_4$ COPR. The Ge(0.5)/$ZnAl_2O_4$ catalysts supported on both $ZnAl_2O_4$ show a wide and poorly defined reduction zone that

Table 2
Activation energies of CHD and Initial reaction rates in CHD and CPH (R^0_{CH}, R^0_{CP}) for Pt, PtSn and PtGe supported on $ZnAl_2O_4$ MS.

Catalyst	Activation energy (kcal/mol)	R^0_{CH} (mol/h g catal.)	R^0_{CP} (mol/h.g catal.)
Pt(0.3 wt.%)/$ZnAl_2O_4$ MS	17	32	0.70
PtSn(0.3 wt.%)/$ZnAl_2O_4$ MS	29	1	n.d.
PtSn(0.5 wt.%)/$ZnAl_2O_4$ MS	25	3	n.d.
PtGe(0.18 wt.%)/$ZnAl_2O_4$ MS	20	5	n.d.
PtGe(0.3 wt.%)/$ZnAl_2O_4$ MS	22	5	n.d.

Table 3
Activation energies of CHD and initial reaction rates in CHD and CPH (R^0_{CH} and R^0_{CP}) for Pt, PtSn and PtGe supported on $ZnAl_2O_4$ COPR.

Catalyst	Activation Energy (kcal/mol)	R^0_{CH} (mol/h.g catal.)	R^0_{CP} (mol/h.g catal.)
Pt(0.3 wt.%)/$ZnAl_2O_4$ COPR	14	72	0.70
PtSn(0.3 wt.%)/$ZnAl_2O_4$ COPR	22	10	n.d.
PtSn(0.5 wt.%)/$ZnAl_2O_4$ COPR	24	6	n.d.
PtGe(0.18 wt.%)/$ZnAl_2O_4$ COPR	25	4	n.d.
PtGe(0.3 wt.%)/$ZnAl_2O_4$ COPR	27	2	n.d.

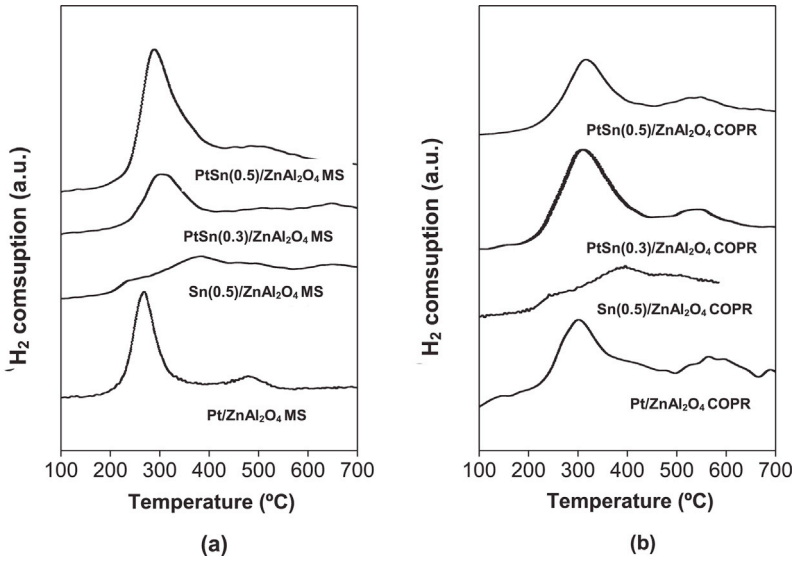

Fig. 4. TPR profiles of (PtSn (0.3 and 0.5 wt.%) catalysts supported on $ZnAl_2O_4$ MS (a) and $ZnAl_2O_4$ COPR (b). TPR of monometallic ones were added as a reference.

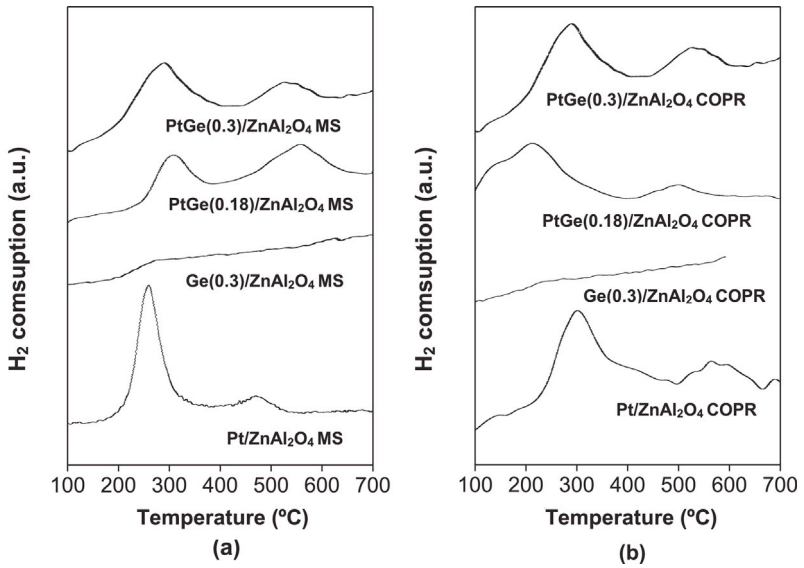

Fig. 5. TPR profiles of (PtGe (0.18 and 0.3 wt.%) catalysts supported on $ZnAl_2O_4$ MS (a) and $ZnAl_2O_4$ COPR (b). TPR of monometallic ones were added as a reference.

Table 4
Total chemisorbed H_2 by Pt, PtSn and PtGe supported on $ZnAl_2O_4$ MS and $ZnAl_2O_4$ COPR.

Catalyst	Total V_{H2} (mL H_2 STP/g catal.)	
	MS	COPR
Pt(0.3 wt.%)/$ZnAl_2O_4$	1.98	3.13
PtSn(0.5 wt.%)/$ZnAl_2O_4$	0.450	0.750
PtGe(0.3 wt.%)/$ZnAl_2O_4$	0.265	0.445

begins at about 200 °C and it is extended up to 700 °C, which could be attributed to the reduction of Ge^{4+} [53] for both supports. In the case of PtGe catalysts supported on $ZnAl_2O_4$ COPR and $ZnAl_2O_4$ MS (Fig. 5) two important reduction zones are observed, the first one with maxima at 220–280 °C and 300 °C, respectively, and the second one has a maximum at about 550 °C for both samples. The main Pt reduction peak in the monometallic catalyst gets wider with Ge addition because of the co-reduction of Pt and Ge with probable alloy formation or a catalytic effect of metallic Pt on the second metal reduction in either case. The second peak could be caused by the reduction of GeOx species in the vicinity of the metallic Pt.

Table 4 shows chemisorption values for different samples. The hydrogen chemisorption of the Pt/$ZnAl_2O_4$ COPR was higher than Pt/$ZnAl_2O_4$ MS. In general it was observed a decrease of the hydrogen chemisorption in the bimetallic catalysts. These results agree with several authors [54–56] that studied Pt and PtSn catalysts supported on Al_2O_3 and the results could be explained by synergy among three important factors: (i) electronic interactions between Pt and Sn with a probable alloy formation, which cannot chemisorb hydrogen, (ii) Sn surface enrichment which partially covers the Pt surface and (iii) blocking/dilution effect of Pt by Sn.

In the case of catalysts supported on $ZnAl_2O_4$ COPR, the second metal addition decreases the hydrogen chemisorptions. The second metal addition could not only form Pt-Sn or Pt-Ge alloys but also cover Pt crystallites with Sn or Ge, thus decreasing the H_2 chemisorption capacity.

Moreover, TEM images of PtSn(0.5)/$ZnAl_2O_4$ MS and PtSn(0.5)/$ZnAl_2O_4$ COPR catalysts are shown in Fig. 6. For the PtGe catalysts that showed a low performance no further studies were done. Fig. 7 shows the particle size distribution (from TEM experiments) of PtSn(0.5)/$ZnAl_2O_4$ MS and PtSn(0.5)/$ZnAl_2O_4$ COPR catalysts. The particle size distributions (from TEM experiments) of PtSn/$ZnAl_2O_4$ MS catalyst were the following: 1–1.5 nm (34%), 1.5–2 nm (40%) and 2–2.5 nm (26%). The TEM characterization of the PtSn(0.5)/$ZnAl_2O_4$ COPR catalyst showed a particle size distribution of: 1–1.5 nm (57%), 1.5–2 nm (40%) and 2–2.5 nm (3.5%). In comparing the particle sizes of bimetallic catalysts with those of the monometallic ones, no noticeable differences were found which would indicate that the chemisorption decrease would not be caused by a particle size effect but electronic and/or geometric effects.

In order to determine the binding energies of Sn3d for PtSn(0.5)/$ZnAl_2O_4$ MS and PtSn(0.5)/$ZnAl_2O_4$ COPR catalysts, and Ge3d for PtGe(0.3)/$ZnAl_2O_4$ COPR catalyst, XPS measurements were done. In both bimetallic catalysts, Pt4f signal had binding energies between 314.1 and 313.6 eV that belongs to metallic Pt. Table 5 shows the binding energies and Sn/Pt and Ge/Pt surface atomic ratios from XPS analysis. It was not possible to discriminate between $Sn3d_{5/2}$ binding energies of Sn(II) and Sn(IV) (486–487 eV) since their values are very close [57]. XPS spectra ($Sn3d_{5/2}$ signal) of PtSn(0.5)/$ZnAl_2O_4$ MS and PtSn(0.5)/$ZnAl_2O_4$ COPR catalysts showed two peaks. Sn would be in two oxidation states: as oxidized Sn species (one portion in contact with Pt, and the other one in contact with the support) and in a lower proportion in zerovalent state, perhaps alloyed with Pt. It was found 26% of metallic Sn for PtSn(0.5)/$ZnAl_2O_4$ MS catalyst and 33% for PtSn(0.5)/$ZnAl_2O_4$

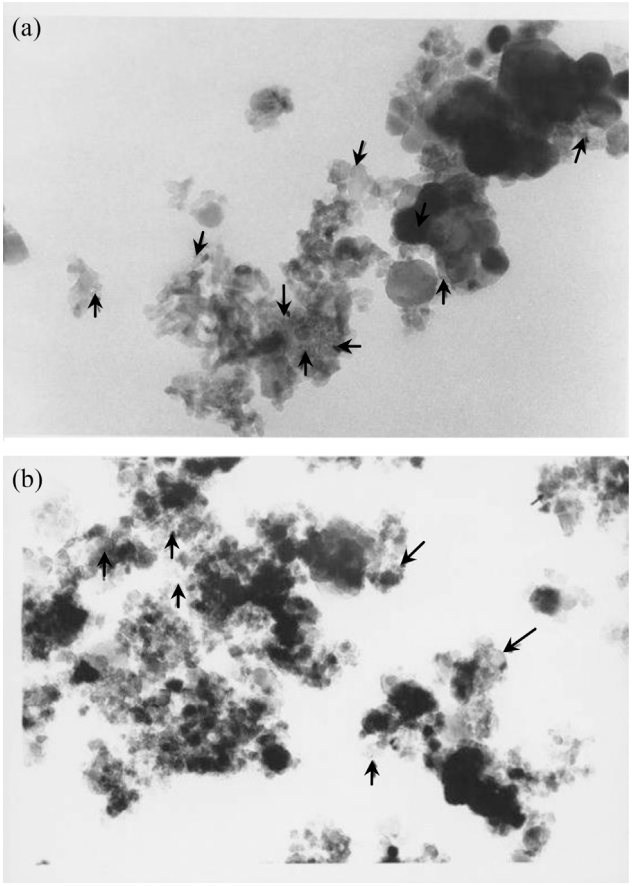

Fig. 6. TEM images of PtSn (0.5 wt.%)/$ZnAl_2O_4$ MS (a) and PtSn (0.5 wt.%)/$ZnAl_2O_4$ COPR catalysts (b).

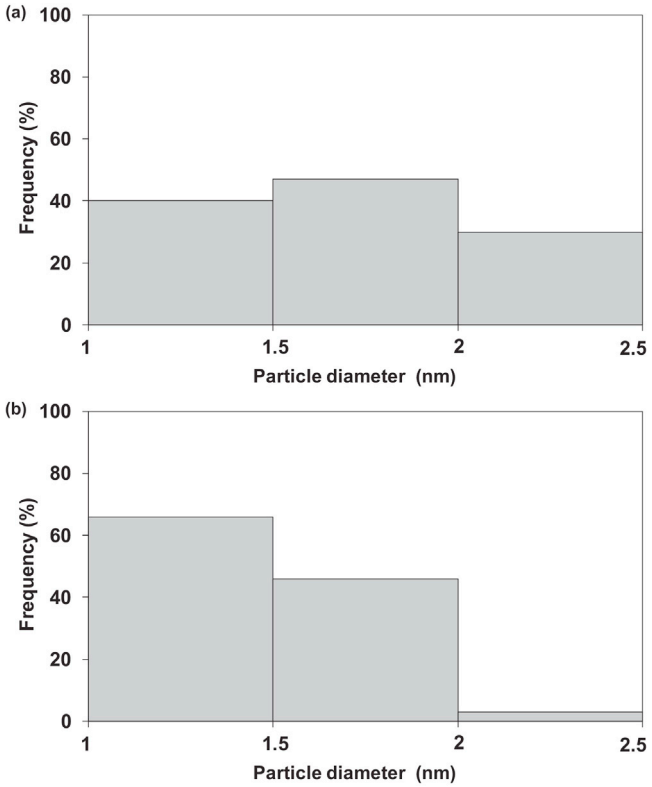

Fig. 7. The particle size distribution of PtSn (0.5 wt.%)/$ZnAl_2O_4$ MS (a) and PtSn (0.5 wt.%)/$ZnAl_2O_4$ COPR catalysts (b).

Table 5
Binding energies (BE) and bulk Sn/Pt and Ge/Pt ratios for the different samples.

Catalyst	Binding energies $Sn3d_{5/2}$ (eV)	Binding energies $Ge3d_{5/2}$ (eV)	Atomic surface ratio Sn/Pt or Ge/Pt
PtSn(0.5 wt.%)/$ZnAl_2O_4$	486.5 (74.1%)		35
MS	484.6 (25.9%)		
PtSn(0.5 wt.%)/$ZnAl_2O_4$	485.8 (66.6%)		36.5
COPR	484.5 (33.4%)		
PtGe(0.18 wt.%)/$ZnAl_2O_4$		30.6 (64%)	28
COPR		32.4 (21%)	
		29.1 (15%)	

COPR catalyst. From Table 5 it can be observed an important surface enrichment of Sn since the Sn/Pt surface atomic ratio is higher, this being 35 for PtSn(0.5)/$ZnAl_2O_4$ MS catalyst and 36.5 for PtSn(0.5 wt.%)/$ZnAl_2O_4$ COPR one.

From XPS, TPR analysis and test reactions it can be concluded that the surface of reduced PtSn catalysts would be conformed by metallic platinum, Sn(II) and/or Sn(IV) in high concentrations (some of them in contact with Pt) and smaller quantities of metallic Sn probably in alloyed phases with metallic Pt. No noticeable differences were found between the behaviour of both supports.

The XPS spectrum (Ge3d signal) was made for PtGe(0.5)/$ZnAl_2O_4$ COPR catalyst. Ge 3d signal has a doublet at 3d3/2 and 3d5/2. It was not possible to determine the difference between Ge(II) and Ge(IV) species since there is a slight difference in their binding energies [58]. Ge3d signal of PtGe(0.3)/$ZnAl_2O_4$ COPR catalyst showed three peaks. A high proportion of Ge is in an oxidized state (Ge(II) (64%) and Ge(IV) (21%)), probably in contact with Pt or with the support, and 15% of Ge would be as Ge(0), probably alloyed to Pt as TPR and test reactions confirm. From Table 5 it can be observed that there is a surface Ge enrichment, since the Ge/Pt surface atomic ratio is 28.

Results of hydrogen chemisorption and cyclohexane dehydrogenation rate would be related to geometric effects of dilution and/or blocking of Pt by Sn and also the formation of alloys or intermetallic Pt-Sn compounds as it was observed from the test reactions rather than a particle size effect as confirmed by TEM. Sn also exists as ionic species stabilized on the support. In the case of PtGe/$ZnAl_2O_4$ catalysts there are both electronic and geometrical (blocking and/or dilution) effects according to activation energy values, R^0_{CH}, R^0_{CP} and hydrogen chemisorption results. These effects reduced the concentration of exposed Pt. The defined reduction signals in TPR for PtGe/$ZnAl_2O_4$ catalyst showed that a fraction of Ge would be segregated and another part would be co-reduced with Pt and forming alloys. There would also be electronic effects as CHD reactions indicate. Besides, the alloyed particles exhibit low dehydrogenation and hydrogenolysis activities.

3.3. Catalytic tests

Fig. 8 shows the initial and final n-decane conversion for bimetallic PtSn and PtGe catalysts supported on $ZnAl_2O_4$ MS and $ZnAl_2O_4$ COPR. The behaviour of monometallic Pt/$ZnAl_2O_4$ MS and Pt/$ZnAl_2O_4$ COPR are also included for comparison. It can be observed that Pt/$ZnAl_2O_4$ COPR and Pt/$ZnAl_2O_4$ MS showed a similar average activity, the initial activity of Pt/$ZnAl_2O_4$ COPR catalyst was slightly higher than that of Pt/$ZnAl_2O_4$ MS. The bimetallic PtSn and PtGe catalysts show a higher activity than the corresponding monometallic Pt ones. It would be expected that the monometallic catalysts were more active than the bimetallic ones at the beginning of the reaction. However, if the carbon deposition in the first step of the reaction is higher in the monometallic catalysts than in bimetallic ones, the initial activity would decrease more rapidly in monometallic than in bimetallic samples. This coke deposition during the first 10 min of reaction time would produce a higher deactivation in Pt monometallic samples. It can be also observed

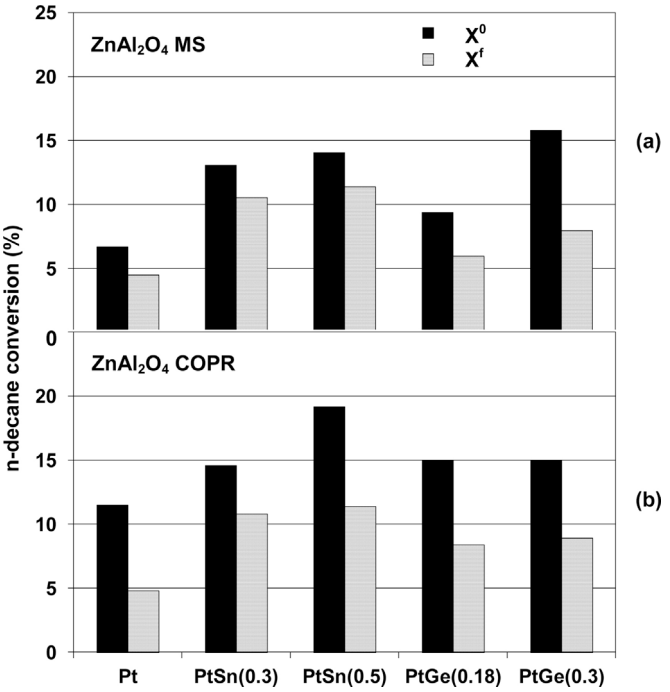

Fig. 8. Initial n-decane conversion $(X^0)^*$ and final n-decane conversion $(X^f)^*$ for PtSn (0.3 and 0.5 wt.%) and PtGe (0.18 and 0.3 wt.%) supported on $ZnAl_2O_4$ MS (a) and $ZnAl_2O_4$ COPR (b). $^*X^0$: at 10 min of the reaction time and X^f: at 130 min of the reaction time.

that the initial activity (n-decane conversion) slightly increases as the Sn content increases for both supports. Similar behavior with respect to Ge content is obtained with the PtGe catalysts. Besides, PtSn catalysts were more active than the PtGe ones. Furthermore, the bimetallic catalysts supported on $ZnAl_2O_4$ COPR were more active than those supported on $ZnAl_2O_4$ MS.

The results of catalyst deactivation measured by the DP values (defined as $DP = 100 \times (X^0 - X^f)/X^0$, where X^0 and X^f are the initial and the final n-decane conversions measured at 10 min and 130 min of the reaction time respectively) are shown in Fig. 9. It can be observed that the Pt/$ZnAl_2O_4$ MS catalyst (DP = 40.6%) has a lower decrease of activity than Pt/$ZnAl_2O_4$ COPR one (DP = 56.6%). This is in agreement with the total C deposited determined by TPO (0.75%C for Pt/$ZnAl_2O_4$ COPR and 0.27%C for Pt/$ZnAl_2O_4$ MS). These results indicate that the coke formation is an important factor in the catalyst deactivation. It must be indicated that Pt/$ZnAl_2O_4$ COPR had higher H_2 chemisorption capacity, higher metallic dispersion and lower particle size than Pt/$ZnAl_2O_4$ MS. This means that Pt/$ZnAl_2O_4$ COPR has an important concentration of Pt sites which are active for dehydrogenation of large paraffins.

In the case of bimetallic catalysts, they had a lower deactivation than the corresponding monometallic ones (except for PtGe (0.3)/$ZnAl_2O_4$ MS). Besides, it can be observed that bimetallic catalysts supported on $ZnAl_2O_4$ COPR had a higher deactivation than the ones supported on $ZnAl_2O_4$ MS. Moreover, PtSn(0.5)/$ZnAl_2O_4$

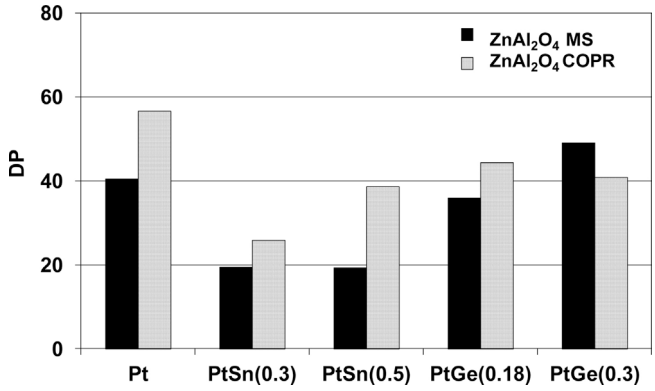

Fig. 9. DP values of Pt, PtSn (0.3 and 0.5 wt.%) and PtGe (0.18 and 0.3 wt.%) catalysts supported on $ZnAl_2O_4$ MS and $ZnAl_2O_4$ COPR.

MS catalyst has the lowest DP, while PtGe(0.3)/$ZnAl_2O_4$ MS sample displays the highest deactivation of all bimetallic catalysts. It could be concluded that all PtGe catalysts showed a higher deactivation than the corresponding PtSn for both supports. This difference is more marked for the bimetallic catalysts supported on $ZnAl_2O_4$ MS. For example, the DP for PtSn(0.5)/$ZnAl_2O_4$ COPR is 38.7% while for PtSn(0.5)/$ZnAl_2O_4$ MS is 19.4%. The addition of a second metal (Sn or Ge) increased the activation energy in CHD, thus indicating an electronic modification probable due to alloys formation. This effect was slightly more pronounced for PtSn catalysts than for PtGe ones when the support MS is used. Minor differences were found in bimetallic catalysts supported on $ZnAl_2O_4$ COPR.

Fig. 10 shows the relationship between DP, previously defined, and the carbon content determined by TPO (at the end of the reaction) for different catalysts. It can be concluded that there is a good correlation between DP and the final coke content for the catalysts supported on $ZnAl_2O_4$ COPR. In the case of catalysts supported on $ZnAl_2O_4$ MS it was not possible to obtain a good correlation between these parameters probably due to the low carbon content.

As it was previously mentioned, undesirable side reactions and coke deposition can be important factors that influence the catalytic

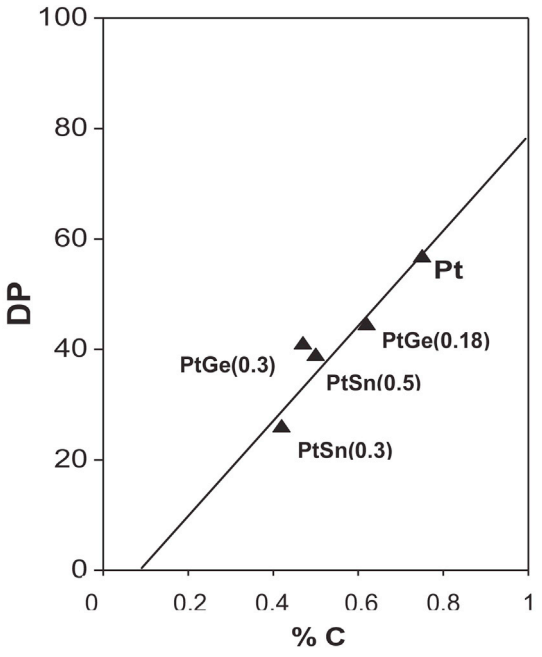

Fig. 10. Relationship between the DP and the final carbon content (C%) for mono and bimetallic PtSn and PtGe catalysts supported on $ZnAl_2O_4$ COPR.

performance since for thermodynamic reasons it is necessary to use high temperatures. When the formed olefin is strongly adsorbed on the metal through π bonds it is possible that the dehydrogenation continues, mainly at low H_2 pressure. It must be also indicated that the polymerization reaction to coke can be catalyzed by both acidic and metallic centers. In the last case the hydrogenolysis reaction is a demanding one being carried out on the same metallic centers than the polymerization [40,59,60] reaction. In the case of monometallic Pt catalysts, the initial deactivation and the coke deposition is very important. These effects appear to be more important in Pt/$ZnAl_2O_4$ COPR than in Pt/$ZnAl_2O_4$ MS. Additional determinations of carbon deposited (by TPO) at 10 min from the beginning of the reaction show a very important initial deposition of coke in monometallic catalysts. In fact, it was found that the initial carbon deposition was about 70% of the total carbon deposited on the catalysts at the end of the reaction for Pt/$ZnAl_2O_4$ MS. This deposited carbon would block the active centers for the hydrogenolisis reaction, thus favouring the dehydrogenation capacity, although the activity decreases. Simultaneously, the catalysts supported on Zn spinels show low coke formation rate since this support would lead to surface metallic structures with low density of edges and corners, which are the active sites for the hydrogenolysis reaction and coke formation [21,51].

The addition of the second metal decreases the amount of deposited carbon with respect to that of the monometallic ones. Besides, the Sn or Ge addition to Pt favours the n-decane dehydrogenation to olefins, minimizing other undesirable reactions, since the electronic and geometric effects (which appear to be slightly higher for Sn than for Ge) are present. These effects can decrease the interaction strength of the olefins with the metallic sites, thus maintaining the metallic surface with low amount of the coke. This effect appears to be more pronounced when the second metal content increases. de Miguel et al. [61] found a similar effect for PtSn and PtGe catalysts supported on Al_2O_3 and MgO. Besides, TPO experiments of the PtSn(0.5)/$ZnAl_2O_4$ MS and PtSn(0.5)/$ZnAl_2O_4$ COPR were made at 10 min of the beginning of the reaction too, and the results showed that the coke deposition was practically negligible (<0.1 wt.%), thus showing that the bimetallic PtSn catalysts had low initial deactivation in contrast to the monometallic ones.

Fig. 11 shows the TPO profiles of Pt supported on $ZnAl_2O_4$ MS and $ZnAl_2O_4$ COPR at the end of the n-decane dehydrogenation reaction. It can be observed that the support has an important effect on the amount of deposited carbon. In fact, it is clearly noted that the Pt/$ZnAl_2O_4$ MS catalyst has lower carbon deposition than Pt/$ZnAl_2O_4$ COPR one. Besides, the TPO of used Pt/$ZnAl_2O_4$ MS shows a burning peak at low temperature, which indicates that an important carbon fraction is deposited on the metal. On the other hand, the Pt/$ZnAl_2O_4$ COPR catalyst shows that carbon is mainly deposited on the support.

Fig. 12 displays TPO profiles taken at the end of n-decane dehydrogenation reaction for PtSn (0.5) (a) and PtGe (0.3) (b) catalysts supported both on $ZnAl_2O_4$ MS and $ZnAl_2O_4$ COPR. It can be observed not only the effect of the support but also the effect of the second metal addition. In the case of PtSn(0.5)/$ZnAl_2O_4$ COPR it is observed a broad peak between 310 and 550 °C, which corresponds to carbon deposited on the metallic function (although in minor proportion) and on the support (in a major quantity) [62–65]. In the case of the PtSn(0.5)/$ZnAl_2O_4$ MS catalyst, it was observed a low amount of carbon deposited on the metallic phase although with low toxicity according to the results above mentioned. From TPO profile of PtGe(0.3)/$ZnAl_2O_4$ COPR catalyst, it can be observed a peak with a maximum at 470 °C which can be attributed to the burning of an important amount of coke mainly deposited on the support [63–66]. In the case of the TPO profile of PtGe(0.3)/$ZnAl_2O_4$ MS, it can be observed a broad peak which begins at low temperature. This result would indicate that the important amount of

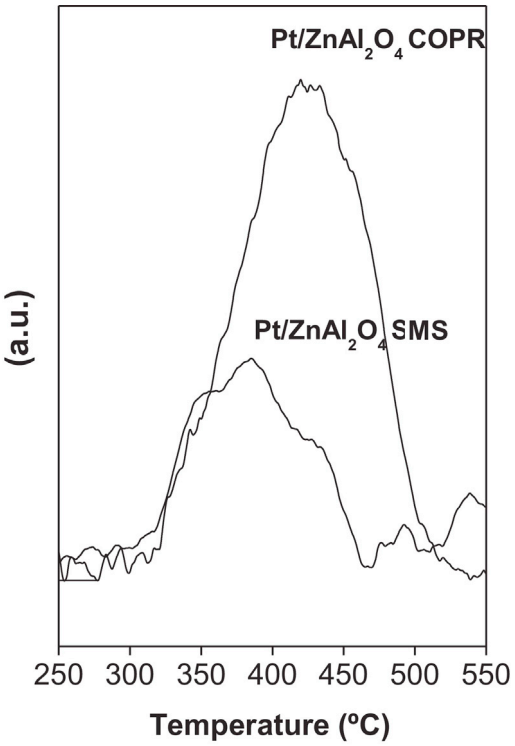

Fig. 11. TPO profiles of Pt supported on $ZnAl_2O_4$ MS and $ZnAl_2O_4$ COPR at the end of the n-decane dehydrogenation reaction.

carbon deposited on the metallic phase and has a different toxicity. In fact, the coke deposited on this catalyst is clearly lower than that deposited on the catalyst supported on $ZnAl_2O_4$ COPR, but their DP is higher than the second one, which means a higher toxicity of the carbon deposited on PtGe(0.3)/$ZnAl_2O_4$ MS catalyst.

Fig. 13 displays the results of average selectivities (along the reaction time) to [$<C_{10}$], [$C_{10=}$] and to [i-c C_{10}] in the n-decane dehydrogenation for mono and bimetallic catalysts supported on $ZnAl_2O_4$ MS y $ZnAl_2O_4$ COPR. It must be noted that it is possible to determine average selectivities since the selectivity to each group of products slightly changes with the reaction time.

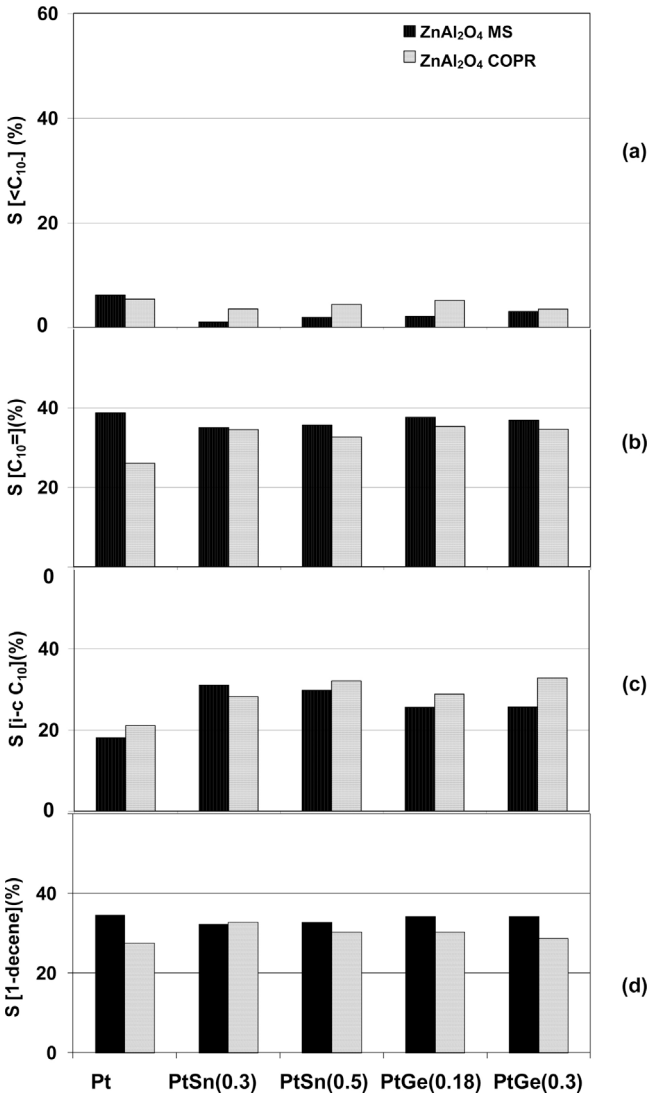

Fig. 13. Average selectivity to [$<C_{10}$] (a), [$C_{10=}$] (b), [i-c C_{10}] (c) and 1-decene (d) in n-decane dehydrogenation for mono and bimetallic catalysts supported on $ZnAl_2O_4$ MS and $ZnAl_2O_4$ COPR.

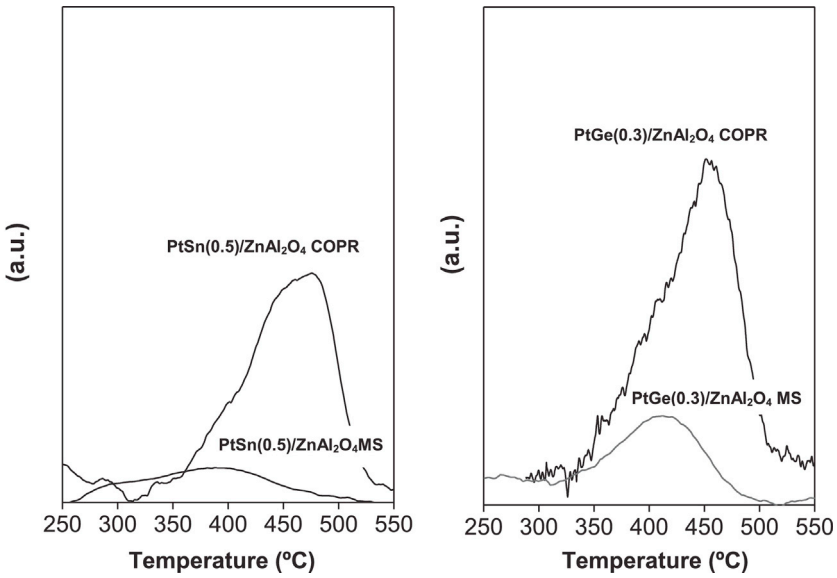

Fig. 12. TPO profiles of PtSn (a) and PtGe (b) catalysts supported on $ZnAl_2O_4$ MS and $ZnAl_2O_4$ COPR after the n-decane dehydrogenation reaction.

Fig. 13a shows the average selectivities (in the reaction time) to [<C_{10}] in the n-decane dehydrogenation for mono and bimetallic catalysts supported on $ZnAl_2O_4$ MS and $ZnAl_2O_4$ COPR. The light paraffins are produced by breaking of C—C bonds, and they can be produced by two ways: (i) cracking via acid sites (cracking of olefins produced by dehydrogenation in the metallic phase) and (ii) hydrogenolysis catalyzed by metallic centers [40,60,61]. Olefins are cracked or isomerized more quickly than linear paraffins. Taking into account the neutral characteristic of the supports, the reactions catalyzed by acid centres have a low participation. It must be noted that the selectivity to [<C_{10}] is practically the same for both Pt monometallic catalysts, which is in agreement with the hydrogenolytic capacity of these catalysts. It should be remembered that the low acidity of both supports does not appear to play an important role in the reaction. It is also observed that Sn or Ge addition to monometallic catalysts produces a decrease of the selectivity to [<C_{10}], this effect being more pronounced for catalysts supported on $ZnAl_2O_4$ MS. Besides, PtSn catalysts are less selective to [<C_{10}] than PtGe ones, mainly those supported on $ZnAl_2O_4$ MS. The lower selectivities to [<C_{10}] of the bimetallic catalyst supported on $ZnAl_2O_4$ MS respect to the one supported on $ZnAl_2O_4$ COPR are due to the higher acidity of the last one. Furthermore, the second metal addition produces a poisoning effect on the acidity [3,60,66], which leads to bimetallic catalysts with low degradation capacity of the raw paraffin.

The average selectivities to other monoolefins (except α-monoolefin), diolefins, dienes, trienes, etc., [$C_{10=}$] are shown in Fig. 13b. It must be indicated that these reactions are very fast and they are produced on the metallic phase. This Figure shows that Pt and bimetallic catalysts supported on $ZnAl_2O_4$ MS have higher selectivities to [$C_{10=}$] than the same catalysts supported on $ZnAl_2O_4$ COPR. Besides, the Sn or Ge addition to Pt/$ZnAl_2O_4$ MS or Pt/$ZnAl_2O_4$ COPR, does not produce an important modification of the selectivity to [$C_{10=}$]. Furthermore, it is also observed that the Sn or Ge loading have slight influence on the selectivity to [$C_{10=}$], and PtGe catalysts were slightly more selective than the PtSn ones, for both supports.

The average selectivities to non-linear chains (including branched chains, isoparaffins, iso-olefins, cyclization products, aromatics, alkyl aromatics) [i-c C_{10}], are shown in Fig. 13c. The aromatization reaction (dehydrocyclization of paraffins) is a fast and structure-sensitive one [40] and it can be produced through a bifunctional mechanism, where the olefins produced on the metal can migrate to the acidic function for a further cyclization. The mechanism of consecutive dehydrogenation, first on the metallic sites and then on the acidic ones can be represented by the following scheme:

n-decane → decene → aromatics
dehydrogenation cyclization

In this group of products [i-c C_{10}] the isomerization products from the original paraffins are included. The isomerization (fast reaction) can be produced on the acidic sites of the supports and in a lower quantity on the metallic sites. It must be noted that the average selectivity to [i-c C_{10}] for the Pt/$ZnAl_2O_4$ MS catalyst is slightly lower than for Pt/$ZnAl_2O_4$ COPR one, and it is favoured by the higher acidity of the support. The average selectivities to [i-c C_{10}] for bimetallic catalysts are higher than those of the corresponding monometallic ones, independently of the support. These surprising results would be not expected, and the explanation of these phenomena is that the average selectivities were calculated after 10 min of the reaction beginning. It must be considered that during the first 10 min of the reaction there is an important deposition of coke (both on the metal phase and the support) in the monometallic samples with respect to the bimetallic ones, which would inhibit in an important way the olefin formation, leading to isomerization and cyclization reactions in the monometallic catalysts and decreasing the selectivity to [i-c C_{10}]. The bimetallic catalysts show opposite effects where the cyclization is less affected than dehydrogenation by the second metal addition. In general, mono and bimetallic catalysts supported on $ZnAl_2O_4$ COPR were more selective to [i-c C_{10}] than those supported on $ZnAl_2O_4$ MS.

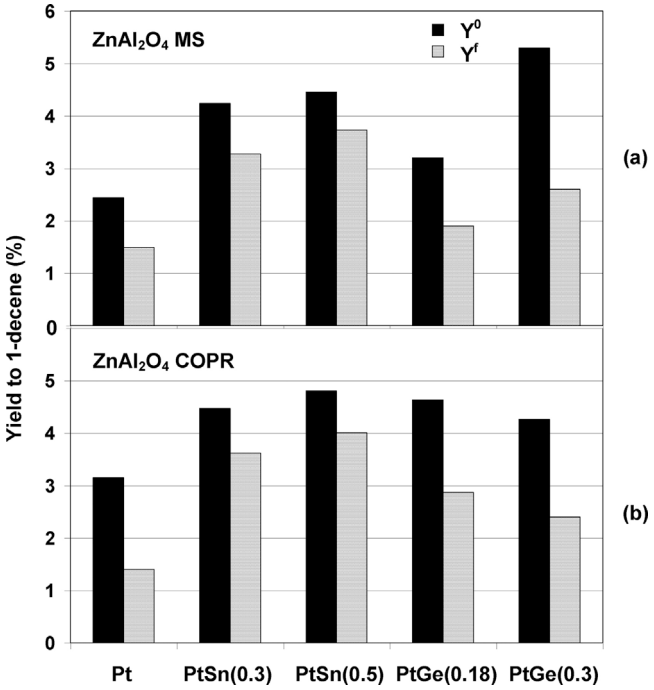

Fig. 14. Initial n-decane yield (Y^0) and final n-decane yield (Y^f)* for mono and bimetallic catalysts supported on $ZnAl_2O_4$ synthesized by MS (a) and COPR (b) methods. (*) Y^0: at 10 min of the reaction time and Y^f: at 130 min of the reaction time.

As regards the average selectivity to 1-decene of the catalysts supported on both $ZnAl_2O_4$ are shown in Fig. 13d. It could be observed that the bimetallic catalysts were more selective to 1-decene than the corresponding monometallic ones supported on $ZnAl_2O_4$ MS and show lower deactivation. The bimetallic catalysts supported on $ZnAl_2O_4$ COPR showed a higher selectivity to 1-decene than monometallic ones.

In analyzing the selectivity to 1-decene of the catalysts with the reaction time, the fall of the initial selectivities in the monometallic catalysts were higher than for the corresponding bimetallic ones, independently of the support. According to Fig. 6 the conversion level for the monometallic catalysts is lower than the bimetallic ones even for the initial conversion. This behaviour can be related to an important carbon deposition on monometallic catalysts in contrast with the lower carbon deposition in the bimetallic systems as it was mentioned. With the Sn or Ge addition to Pt, the selectivity to 1-decene mainly in the catalysts supported on $ZnAl_2O_4$ MS is increased. Sn and Ge produce electronic-geometric modifications of the metallic phase leading to a decrease of the hydrogenoltic capacity, thus increasing the selectivity to 1-decene. Besides, the lower acidity of $ZnAl_2O_4$ MS favours the dehydrogenation since it decreases the side undesirable reactions, like hydrocraking and polimerization. Moreover, the addition of a second metal (Sn or Ge) to Pt would lead to a weak interaction olefins-metallic phase [3,51,62], which inhibits the consecutive dehydrogenation of the monoolefin. This could be attributed to the modification of Pt ensembles by Sn or Ge (geometric and electronic effects), which decreases the olefins adsorption strength, thus avoiding the subsequent transformation into dienes.

Fig. 14 shows initial and final yields to 1-decene (Y, Y = conversion × selectivity to 1-decene; Y^0: initial, at 10 min of reaction time and Y^f: final, at 130. min of the reaction beginning)

for different mono a bimetallic catalysts supported on $ZnAl_2O_4$ COPR and $ZnAl_2O_4$ MS. It can be observed that the $Pt/ZnAl_2O_4$ COPR catalyst has a higher yield to 1-decene than $Pt/ZnAl_2O_4$ MS one, although the final yields of both catalysts are similar. The bimetallic catalysts show higher yields with respect to those of the monometallic ones for both supports. However, PtGe catalysts have higher yields when the support is $ZnAl_2O_4$ COPR. This effect could be explained by the high conversion of these samples. Moreover, for both support types, the yield to 1-decene is higher for PtSn catalysts than for PtGe ones. With reference to the effect of the second metal loading on the yield to 1-decene, it is observed a positive one when the loading increases.

$PtSn(0.5)/ZnAl_2O_4$ MS catalyst has a yield to 1-decene slightly lower than that of $PtSn(0.5)/ZnAl_2O_4$ COPR one, although the first catalyst is more stable with the reaction time and it has a lower deactivation. These characteristics determine a good catalytic formulation. The higher initial and final yields to 1-decene of $PtSn/ZnAl_2O_4$ COPR catalyst could be due to the more efficient promoter action of Sn which inhibits the undesirable side reactions due to geometric and electronic interactions.

4. Conclusions

It was possible to obtain $ZnAl_2O_4$ by mechanochemical synthesis (MS) or coprecipitation (COPR) with good surface area and low acidity to minimize subsequent reactions of the monoolefins formed during the n-decane dehydrogenation and low coke formation rate since these support surfaces lead to metal structures probably scattered on edges and corners. From the metallic characterization, $PtSn/ZnAl_2O_4$ catalysts showed geometric effects of dilution and/or blocking of Pt by Sn and also the formation of alloys or intermetallic Pt-Sn compounds. In the case of $PtGe/ZnAl_2O_4$ catalysts there were both electronic and geometrical (blocking and/or dilution) reducing the concentration of exposed Pt. A Ge fraction would be segregated and another part would be co-reduced with Pt and forming alloys. Bimetallic catalysts were more active than monometallic ones with lower deactivation. PtSn catalysts on both spinels were more active, with lower activity fall than PtGe ones and the higher the Sn loading, the more noticeable this effect. Besides, PtSn catalysts supported on $ZnAl_2O_4$ MS showed a more stabilizing effect.

Acknowledgements

The authors wish to acknowledge the financial support received from Universidad Nacional del Litoral and ANPCYT-Argentina. They also thank Technician Miguel Torres for his experimental assistance.

References

[1] UOP pacol dehydrogenation process, Peter R. Pujadó, UOP LLC Des Plaines, Illinois, Copyright© 2004, 1997, 1986 by The McGraw-Hill Companies, Inc., McGraw-Hill.
[2] A.K. Kocal, B.V. Vora, T. Imai, Appl. Catal. A: Gen. 221 (2001) 295–301.
[3] A.A. Castro, Catal. Lett. 22 (1993) 123–133.
[4] N.M. Podkletnova, S.B. Kogan, G.B. Bursian, Neftekhimiya 60 (9) (1987) 2028.
[5] G.D.T. Gokak, A.G. Basrur, D. Rajeswar, G.S. Rao, K.R. Krishnamurthy, React. Kinet. Catal. Lett. 59 (2) (1996) 315–323.
[6] D. Sterligov, G.V. Isagulyants, Petrol Chem., U.R.S.S. 3 (20) (1980) 134–140.
[7] B. Kogan, N.M. Podletnova, O.M. Oranskaya, I.V. Semenskaya, N.R. Bursian, Kinet. Katal. 22 (3) (1981) 663–667.
[8] G. García Cortez, S.R. de Miguel, O.A. Scelza, A.A. Castro, Iberoamerican Symposium of Catalysis, Segovia, Vol. 1, 1992, pp. 379–382.
[9] G. Padmavathi, K.K. Chaudhuri, D. Rajeshwer, G. Sreenivasa Rao, K.R. Krishnamurthy, P.C. Trivedi, K.K. Hathi, N. Subramanyam, Chem. Eng. Sci. 60 (2005) 4119–4129.
[10] D. Sanfilippo, I. Miracca, Catal. Today 111 (2006) 133–139.
[11] G.J. Antos, A. Arlington UOP Inc. (des Plaines, IL) United States Patent: 4079097 (1978).
[12] N.J. van der Laag, M.D. Snel, P.C. Magusin, G. de With, J. Eur. Ceram. Soc. 24 (2004) 2417–2424.
[13] M. Valenzuela, J. Jacobs, P. Bosch, S. Reijne, B. Zapata, H. Brongersma, Appl. Catal. A: Gen. 148 (1997) 315–324.
[14] Valenzuela MA (1990) Thesis, ESIQIE-IPN, México.
[15] B. Strohmeier, D. Hercules, J. Catal. 8 (1984) 266–279.
[16] I. Ganesh, B. Srinivas, B. Saha, R. Johnson, Y. Mahajan, J. Eur. Ceram. Soc. 24 (2004) 201–207.
[17] M.V. Zdujié, O.B. Milosevié, Mater. Lett. 13 (1992) 125–129.
[18] D. Domanski, G. Urretavizcaya, F. Castro, F. Gennari, J. Am. Ceram. Soc. 87 (2004) 2020–2024.
[19] L.B. Kong, J.M. Huang, Mater. Lett. 56 (2002) 238–243.
[20] T. El-Nabharawy, A. Attia, M. Alaya, Mater. Lett. 24 (1995) 319–325.
[21] G. Aguilar-Rios, M.A. Valenzuela, Appl. Catal. A: Gen. 90 (1992) 25–34.
[22] H. Armendariz, A. Guzmán, A. Toledo, M. Llanos, A. Vazquez, G. Aguilar, in: J. Morfao, J. Faria, J. Figueiredo (Eds.), Proc. XVII Iberoamerican Symposium of Catalysis, Porto, 2000, pp. 105–114.
[23] J.G. Li, T. Ikegami, J. Lee, T. Mori, Y. Yamija, Ceram. Int. 27 (2001) 481–489.
[24] J. Li, T. Ikegami, J. Lee, T. Mori, Y. Yajima, J. Eur. Ceram. Soc. 21 (2001) 139–148.
[25] J. Guo, H. Lou, X. Wang, X. Zheng, Mater. Lett. 58 (2004) 1920–1923.
[26] L. Chen, X. Sun, J. Alloys Compd. 376 (2004) 257–261.
[27] Y. Wu, J. Du, K. Leong Choy, L. Hench, J. Guo, J. Thin Solid Film 472 (2005) 150–156.
[28] G. Monrós, J. Tena, J. Mater. Chem. 5 (1995) 85–90.
[29] M. Zawadzki, Solid State Sci. 8 (2006) 14–18.
[30] J. Wrzyszcz, M. Zawadzki, J. Mol. Catal. A: Chem. 189 (2002) 203–210.
[31] M. Zawadzki, W. Mista, L. KepinskiL, Vacuum 63 (2001) 291–296.
[32] Z. Chen, E. Shi, Mater. Lett. 56 (2002) 601–605.
[33] C.C. Yang, S.Y. Chen, S.Y. Cheng, Powder Technol. 148 (2004) 3–6.
[34] T. Mimani, J. Alloys Compd. 315 (2001) 123–128.
[35] Z. Li, S. Zhang, W. Lee, J. Eur. Ceram. Soc. 27 (2007) 3407–3412.
[36] A.D. Ballarini, S.A. Bocanegra, A. Alberto, S.R. Castro, O.A. de Miguel, Scelza, Catal. Lett. 129 (2009) 293–302.
[37] M.E. Olbrich, J.H. Kolts, presented at the AICHE Spring National Meeting, New Orleans, Lousiana, Apri16–10 (1980).
[38] R.J. Rennard, J. Freel, J. Catal. 98 (1986) 235.
[39] G. Aguilar Rios, M.A. Valenzuela, H. Armendariz, J.M. Dominguez, D.R. Acosta, I. Schifter, Appl. Catal. A: Gen. 90 (1992) 94.
[40] M. Bhasin, J. McCain, B. Bora, T. Imai, P. Pujadó, Appl. Catal. 221 (2001) 397–419.
[41] M. Roman-Marinez, D. Cazorla-Amoros, A. Linares-Solano, C. Salinas Martinez de Lecea, H. Yamashita, M. Anpo, Carbon 33 (1995) 3–13.
[42] JCPDS file 05-0669.
[43] H. Pines, W. Haag, J. Am. Chem. Soc. 82 (1960) 2471–2478.
[44] N.A. Pakhomov, R.A. Buyanov, Stud. Surf. Sci. Catal. 91 (1995) 1101–1110.
[45] A.D. Cinneide, J.K.A. Clarke, Catal. Rev. 7 (1972) 213–231.
[46] A.A. Balandin, Zh. Fiz. Khimi. 31 (1957) 745–753.
[47] J. von Schaik, R. Desing, V. Ponec, J. Catal. 38 (1975) 293.
[48] M. Boudart, Adv. Catal. 20 (1969) 153.
[49] F.G. Gault, Adv. Catal. 30 (1981) 1.
[50] B. Biloen, J.N. Helle, H. Verbeek, F.M. Dautzembverg, W.M.H. Sachtler, J. Catal. 51 (1980) 112.
[51] G. Aguilar, Ríos-M.A. Valenzuela, D.R. Acosta, I. Shifter, in: L. Guczi, et al. (Eds.), Proceeding of the 10th International Congress on Catalysis, Hungary, 1992, p. 1831.
[52] S.A. Bocanegra, S.R. de Miguel, A.A. Castro, O.A. Scelza, Appl. Catal. A 277 (2004) 1–22.
[53] R. Mariscal, J. Fierro, J. Yori, J. Parera, J. Grau, Appl. Catal. A: Gen. 327 (2007) 123–131.
[54] K. Balakrishnan, J. Schwank, J. Catal. 127 (1991) 287.
[55] A.C. Muller, P.A. Engelhard, J.E. Weisang, J. Catal. 56 (1979) 65–72.
[56] H. Volter, G. Lietz, React. Kinet. Catal. Lett. 16 (1981) 87.
[57] L. Yong-Xi, J. Stencel, B. Davis, React. Kinet. Catal. Lett. 37 (1988) 2.
[58] J. Parera, N. Fígoli, E. Traffano, J. Beltramini, E. Martinelli, Appl. Catal. 5 (1983) 33–38.
[59] J.M. Parera, N.S. Fígoli, G.J. Antos, A.M. Aitani, J.M. Parera (Eds.), Catalytic Naptha Reforming: Science, Tecnology, Marcel Dekker Inc, New York, 1995.
[60] G. García Cortéz, Thesis, INCAPE-FIQ-UNL, Argentina (1992).
[61] S. de Miguel, A.A. Castro, O. Scelza, J.L. García Fierro, J. Soria, Catal. Lett. 36 (1996) 201–206.
[62] J. Barbier, P. Marecot, N. Martin, L. Elassal, R. Laurel, in: B. Delmon, G.F. Froment (Eds.), Catalyst Deactivation, Elsevier Publ. Co, Amsterdam, 1980, p. 53.
[63] F. Carusso, E.L. Joblonski, J.M. Grau, J.M. Parera, Appl. Catal. 61 (1989) 195–202.
[64] B.B. Zharkov, L.B. Galperin, V.L. Medzkinskii, L. Boutochnikova, A.N. Frasilnikov, I.D. Yukova, React. Kinet. Catal. Lett. 32 (1986) 457.
[65] J. Barbier, E.J. Churin, J.M. Parera, J. Rivieri, React. Kinet. Catal. Lett. 29 (1985) 323.
[66] I. Coleto, R. Roldán, C. Jiménez Sanchidrián, J.P. Gómez, F. Romero Salguero, Catal. Today 149 (2010) 275.